Reversal of long-term dendritic spine alterations in Alzheimer disease models

Donna L. Smith[1,2], Julio Pozueta[1], Bing Gong[3], Ottavio Arancio, and Michael Shelanski[4]

Taub Institute for Research on Alzheimer's Disease and the Aging Brain and Department of Pathology and Cell Biology, Columbia University, New York, NY 10032

Synapse loss is strongly correlated with cognitive impairment in Alzheimer's disease (AD). We have previously reported the loss of dendritic spines and the presence of dystrophic neurites in both the hippocampi of transgenic mice overexpressing amyloid precursor protein (APP) and in the human brain affected with AD. In the studies reported here we have asked whether the acute alterations in dendritic spines induced by Aβ, as well as the chronic loss of spine density seen in hAPP transgenic mice, are reversible by treatments that restore the cAMP/PKA/CREB signaling pathway or proteasome function to control levels. The results show that both rolipram and TAT-HA-Uch-L1 restore spine density to near control conditions, even in elderly mice. The results suggest that changes in dendritic structure and function that occur after Aβ elevation are reversible even after long periods of time, and that one could envision therapeutic approaches to AD based on this restoration that could work independently of therapies aimed at lowering Aβ levels in the brain.

Alzheimer disease | memory deficit | synaptic plasticity

Alzheimer's disease (AD) is the most common cause of dementia in elderly individuals. Brain regions involved in learning, memory, and emotional behaviors (namely, the entorhinal cortex, hippocampus, basal forebrain, and amygdala) are reduced in size in AD patients as a result of the degeneration of synapses and, ultimately, the death of neurons (1). The molecular pathological hallmarks of AD are intracellular neurofibrillary tangles and extracellular amyloid (Aβ) plaques (2). The Aβ plaques arise from specific processing of the amyloid precursor protein (APP) that is regulated by the presenilins (PS1 and PS2) (3). The development of Aβ plaques has been successfully achieved in transgenic mice overexpressing mutated forms of APP (4) and is greatly accelerated in transgenic models overexpressing mutated forms of both APP and PS1 (5). APP/PS1 mice display impaired LTP, spatial working memory, and contextual learning as early as 3–4 months of age, and they show deficits in basal synaptic transmission (BST) and spatial reference memory after 5–6 months of age (6).

Human studies have shown significant synaptic pathology in AD (7, 8) and have identified synapse loss as a major correlate of cognitive impairment in the disease (9). Studies in APP transgenic mice have shown functional deficits and synaptic loss before the onset of Aβ plaque formation (10–12). Aβ deposition also results in local synaptic abnormalities and breakage of neuronal branches (14). In APP transgenic mice, one of the earliest morphological changes is a reduction of hippocampal volume because of a loss of dendritic mass (14). Finally, Aβ itself is capable of impairing synaptic plasticity independent of plaque formation both in slices and *in vivo* (15–18)

Dendritic spines are cellular compartments containing the molecular machinery important for synaptic transmission and plasticity (19). In healthy mice, the number of spines on a particular dendrite predicts the number of excitatory synapses and spines with larger heads are thought to have stronger synapses (20–22). Longer spines have synapses that are less mature and more modifiable (23, 24). Examination of *post mortem* brains from AD patients has shown a loss of dendritic spines (25, 26). Dendritic spine loss is also seen in the brains of PDAPP, Tg2576, and J20 APP transgenic mice (27,

28) and in hippocampal slices treated with Aβ (29, 30). Similar results have since been reported by several other groups (28, 31–33)

Over the past several years, Aβ has been demonstrated to inhibit hippocampal long-term potentiation (LTP) and activation of the PKA/CREB pathway in both cultured neurons and murine hippocampal slices (19). Inhibition of LTP is also seen in hippocampal slices taken from APP/PS1 double transgenic mice. This inhibition can be reversed by increasing cAMP with agents such as rolipram or by elevating the intracellular levels of the enzyme ubiquitin c-terminal hydrolase L1 (Uch-L1) (7, 34). Uch-L1 removes ubiquitin from ubiquinated proteins, allowing them to be degraded by the proteasome and the monoubiquitin to be recycled. Both rolipram and a transducible form of Uch-L1 (V-Uch-L1) ameliorate LTP inhibition and behavioral deficits in APP/PS1 transgenic mice when administered i.p. These results raise the question as to whether these effects are mediated by or reflected in the architecture of the dendrites and their spines and, if they are, whether the changes are reversible at all ages or only early in the disease process.

In the work presented here, we have examined dendritic architecture in the hippocampus and, for comparison in the striatum, an area of the brain with little or no Aβ deposition, in APP/PS1 mice at various ages. In addition, acute hippocampal slices have been used to measure the effects of the direct application of oligomeric Aβ on neuronal dendrites and their spines. We have found a decrease in spine density and alterations in spine morphology by direct application of Aβ to wild-type hippocampal slices. These changes were reversed by treatment with either rolipram or V-Uch-L1. More remarkably, the progressive loss of spine density in APP/PS1 transgenic mice was reversed by short-term systemic treatment with these agents in mice as old as 15 months.

Results

Reversibility of Aβ-Induced Spine Alterations in Normal Murine Hippocampal Slices. Hippocampal slices were generated from 4-month-old wild-type (WT) mice, placed on culture membranes, and incubated at 37 °C, 5% CO_2 for 90 min in medium to recover. At that time, 100 nM oligomeric Aβ_{1-42} was added either alone or together with either V-Uch-L1 (20 nM or 100 nM) or rolipram (1 μM or 10 μM) for 24 h. Slices were subsequently fixed, labeled by DiOlistics, and imaged, and dendritic spine parameters were measured (Fig. 1). A 100-nM quantity of Aβ was found to significantly reduce spine density and to alter spine morphology within 24 h.

The exposure of normal hippocampal slices to 100 nM Aβ for 24 h resulted in a 22% decrease in total dendrite area ($P = 0.05$), a 35% decrease in mean dendritic diameter ($P < 0.0001$), and, most
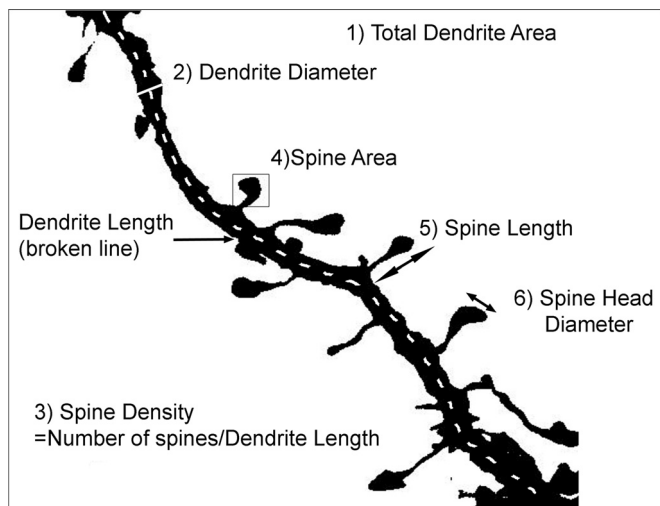
PHYSIOLOGY

Fig. 1. Neuronal dendrite and spine measurement by Image J analysis. A typical dendrite segment from a pyramidal neuron is shown, and the six quantification parameters labeled as follows. 1) Total dendrite area is measured by drawing a box around the whole image; 2) dendrite diameter is obtained by drawing a line across the dendrite thickness at a place of average width; 3) spine density is the total number of spines divided by the dendrite length; 4) spine area is measured by drawing a box around the whole spine; 5) spine length uses the broken line tool to measure the length; and 6) spine head diameter again uses the broken line tool in Image J to measure the diameter across the head of the spine.

dramatically, a 56% decrease in spine density ($P < 0.0001$) (Fig. 2). Both spine area ($P < 0.0001 + 49\%$) and spine head diameter ($P < 0.0001 + 37\%$) were significantly increased, suggesting that synaptic scaling might occur. This phenomenon postulates that the total strength of synaptic output to a given neuron is conserved so that the neuronal output is buffered against disturbances (39). If synaptic scaling is occurring, then there should be a negative correlation between the spine density of a given dendritic segment and the mean spine head diameter of that segment. However, although there was a negative correlation between spine head diameter and spine density in these slices, it did not reach significance (Pearson correlation coefficient $r = -0.56$, $P = 0.790$). Similar results are seen in primary hippocampal neurons treated with 300 nM Aβ, in which a 50% decrease in dendritic spines and an increase in Rho-GTP are seen after 24 h. This argues that the effects of Aβ are directly on the neuron and not mediated by other cells in the tissue.

When V-Uch-L1 was added to Aβ-treated WT slices spine density was increased at concentrations of 20 nM (62%) and 100 nM (66%) as compared with slices treated with Aβ alone (Fig. 2). However, neither total dendrite area or dendrite diameter showed a significant response at 20 nM, whereas 100 nM V-Uch-L1 increased total dendrite area by 50% and dendritic diameter by 34%. Consistent results were obtained when rolipram was added to Aβ treated WT slices. Spine density was increased by 32% by 1 μM ($P = 0.45$) and 42% by 10 μM rolipram ($P = 0.013$). No significant changes in total dendrite area or diameter were seen and, once again, there was a suggestion of synaptic scaling that fell short of statistical significance (Pearson correlation coefficient $r = -0.324$, $P = 0.057$). Treatment with V-Uch-L1 or rolipram in the absence of Aβ did not significantly alter any of the measured parameters.

Age-Dependent Alterations in Dendrites and Dendritic Spines in the APP/PS1 Mouse. The dendrites of pyramidal neurons in the hippocampus and medium and large spiny neurons in the striatum of double transgenic APP/PS1 mice and WT littermate controls were examined at 1, 4, and 14–15 months of age ($n = 3$ for each) using DiOlistic labeling and confocal microscopy. These points were chosen as representative of (*i*) the period before Aβ deposition, (*ii*) the time of early plaque formation and, finally, (*iii*) the stage of severe parenchymal involvement. The hippocampus was chosen because of its alterations in AD, whereas the striatum is not severely affected in the disease.

At 1 month of age, total dendrite area, dendrite diameter, spine density, spine area, and spine head diameter did not differ between control and double transgenic animals, but spine length was increased by 10% ($P < 0.0001$) in APP/PS1 mice compared with WT controls (Fig. 3). At 4 months of age, there was a 30% reduction in spine density ($P < 0.0001$) as well as reductions of $\approx 20\%$ in both dendritic area and dendritic diameter ($P = 0.024$) in the double transgenic mice as compared with controls. These changes are more pronounced at 14–15 months of age where spine density is reduced by 70% and dendrite diameter and dendrite area are decreased by 52% and 61% respectively ($P < 0.0001$ for all values). There were no significant changes in spine area or spine length and only a small difference in spine head diameter between the two groups of animals at 4 months of age. However, at 14–15 months, spine area is increased by 46% ($P < 0.0001$) and spine head diameter by 26% ($P < 0.0001$) in the APP/PS1 mice, whereas spine length remained unchanged from the WT. Spines, therefore, appear to become larger in the older APP/PS1 mice, whereas the density of spines is markedly decreased. The opposing changes seen in spine density and spine head diameter at 14–15 months of age between APP/PS1 and WT mice are consistent with "synaptic scaling," and the spine density shows a significant negative correlation with spine head diameter (Pearson correlation coefficient, $r = -6.26$, $P < 0.0001$). This suggests that, as spines are lost, the remaining spines attempt to compensate by an increase in their size. In contrast to the hippocampal changes in the transgenic mice, the medium and large spiny neurons of the striatum were unchanged at all ages.

The appearance of Aβ plaques in APP/PS1 mice coincides with or comes after the onset of dendrite and spine abnormalities. Aβ plaques were detected in 4-month-old APP/PS1 mice, at the same time that quantification data report that dendrite area, diameter, and spine density were all significantly reduced. At 14–15 months, many more Aβ plaques were observed in the APP/PS1 mice, together with larger alterations in the dendrites and the dendritic spines. No Aβ plaques were detected in 1-month-old APP/PS1 mice or in WT animals.

Reversal of Synaptic Pathology in APP/PS1 Mice by Rolipram and V-Uch-L1. We next examined the effects of rolipram and V-Uch-L1 on the dendritic morphology in the APP/PS1 and WT animals. By doing so, we could determine whether rolipram- and V-Uch-L1-induced recovery of spine density and dendritic architecture observed in Aβ-treated wild-type slices occur and persist in the intact animal. APP/PS1 and WT mice were injected s.c. with rolipram (0.03 mg/kg) or V-Uch-L1 (0.03 mg/kg) daily for 3 weeks starting at either 3 months of age or at 15 months of age. At the end of 3 weeks, pairs of V-Uch-L1 injected, rolipram-injected, and vehicle-injected APP/PS1 mice were killed and analyzed. Wild-type mice treated in the same manner were examined starting at 3 months of age to determine baseline spine densities and whether these densities were altered by either treatment.

Both V-Uch-L1 and rolipram increased the spine density in the 3-month-old treated animals to close to control values ($+29\%$ for rolipram, $P < 0.003$ and $+ 36\%$ for V-Uch-L1, $P < 0.001$) (Fig. 4*A*). Total dendrite area and dendrite diameter were also increased by 25–35%. The shapes of the larger dendritic spines of the V-Uch-L1-treated APP/PS1 mice were not significantly different from controls, but spine length was increased. Rolipram-treated APP/PS1 mice, however, had significant increases in spine area (30%, $P < 0.0001$), spine length (22%, $P = 0.005$), and spine head diameter (15%). Examination of the 15-month-old APP/PS1 animals showed very similar results on spine density, dendrite area, dendrite diameter, and spine head diameter. At 3 months of age, Uch-L1 had no effect on spine area, whereas this agent was
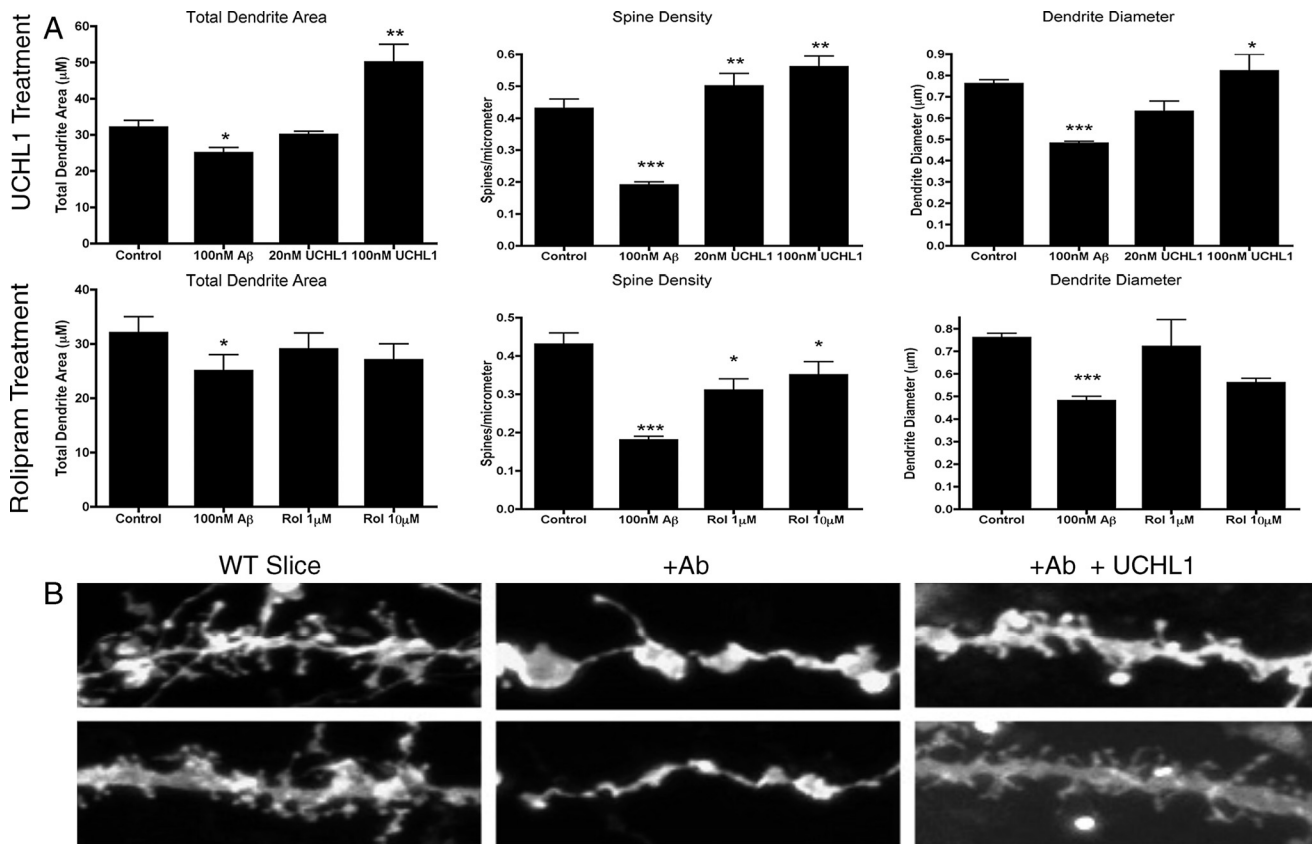
Fig. 2. (*A Upper*) Acute WT hippocampal slices treated with Aβ and V-Uch-L1. Upon addition of Aβ to the WT slices, dendrite area, dendrite diameter, and spine density were all significantly reduced when compared with those of untreated controls. Addition of Uch-L1 (in the continued presence of Aβ) to the Aβ-treated slices reversed these changes by significantly increasing dendrite area and diameter at 100 nM UCHL1 and elevating spine density at both 10 and 100 nM Uch-L1. Spine morphologies were also changed by Aβ. Both spine area and head diameter were increased by the addition of Aβ, and the effect was reversed by Uch-L1 (*, $P < 0.05$, **, $P < 0.005$, ***, $P < 0.0001$). (*A Lower*) As in *Upper*, addition of Aβ to the WT slices reduces dendrite area and diameter as well as spine density when compared with those in untreated controls. Addition of rolipram to the treated Aβ slices elevated spine density for both rolipram concentrations. Both spine area and spine head diameter were increased by Aβ addition, and the effect was reversed by rolipram. (*B*) Examples of dendrite and spine morphologies of pyramidal hippocampal neurons used for quantification. Decreases in dendrite area, diameter, and spine density can clearly be seen when Aβ is added. Uch-L1 reverses the effects of Aβ so that dendrites and spines look more like untreated WT slices. Scale, 10 μm. Similar results (not shown) were obtained with rolipram.

associated with an increased in spine area at 15 months. The differences in spine area may reflect the different mechanisms of action of rolipram and Uch-L1, and could explain the fact that only rolipram improves contextual fear learning the day after training in these mice whereas V-Uch-L1 improves retention of this learning over time (34). Neither Uch-L1 or rolipram had significant effects in the WT animals.

Discussion

Numerous changes in dendritic architecture have been observed, including loss of dendritic spines in transgenic mice overexpressing APP and in the brains of persons dying of AD (27). The studies of Terry (9) show that synaptic loss correlates well with the degree of dementia in humans; similar synaptic loss occurs in advance of significant amyloid deposition in transgenic mice (40).

Although it has been suspected for some time that alterations of dendrites and their spines may play a role in AD, until recently the difficulty of Golgi staining and the lack of animal models has limited studies of dendritic architecture. The introduction of ballistic labeling methods using membrane-soluble dyes has enabled us to examine dendritic spines in a rapid, relatively reproducible manner.

The alterations in dendritic architecture seen in these experiments parallel closely the inhibition of LTP and the development of behavioral deficits in APP/PS1 animals. The changes confirm our earlier studies showing similar changes in both J20 single transgenic and APP/PS1 double transgenic animals and in human AD brain (1). The fact that similar changes can be seen with the direct application of Aβ on slices and on purified hippocampal neurons suggests that these effects are caused by the direct effect of Aβ on neurons rather than by other effects of the transgene(s) or the effects of Aβ acting on other cell types.

Two notable aspects of these experiments are the rapidity with which these changes occur after the addition of Aβ and the ability of rolipram and Uch-L1 to reverse long-standing changes. The physiological alterations are present within 20 min of exposure, and the dendritic changes are extensive within 24 h. These changes are blocked by either rolipram or V-Uch-L1. Although we have examined adult brains in these studies, similar effects (i.e., decreases in dendritic spine density, an increase in spine length, and a suppression of spine motility) are seen in GFP-labeled living neonatal slices exposed to 200 nM Aβ and imaged by 2-photon microscopy. These changes reverse rapidly with rolipram and, more slowly (within 4 days) on the wash-out of Aβ (30).

A consistent result of all of our studies, whether using transgenic animals, human AD brain, or slices treated with exogenous Aβ, is that the loss of synaptic spine density is always partial (≈50% in most cases). This suggests either that there are two populations of spines, one of which is resistant to Aβ, or that the main effect of Aβ is an increase in the rate of spine retraction or a decrease in the rate of spine formation, establishing a new equilibrium between the two.
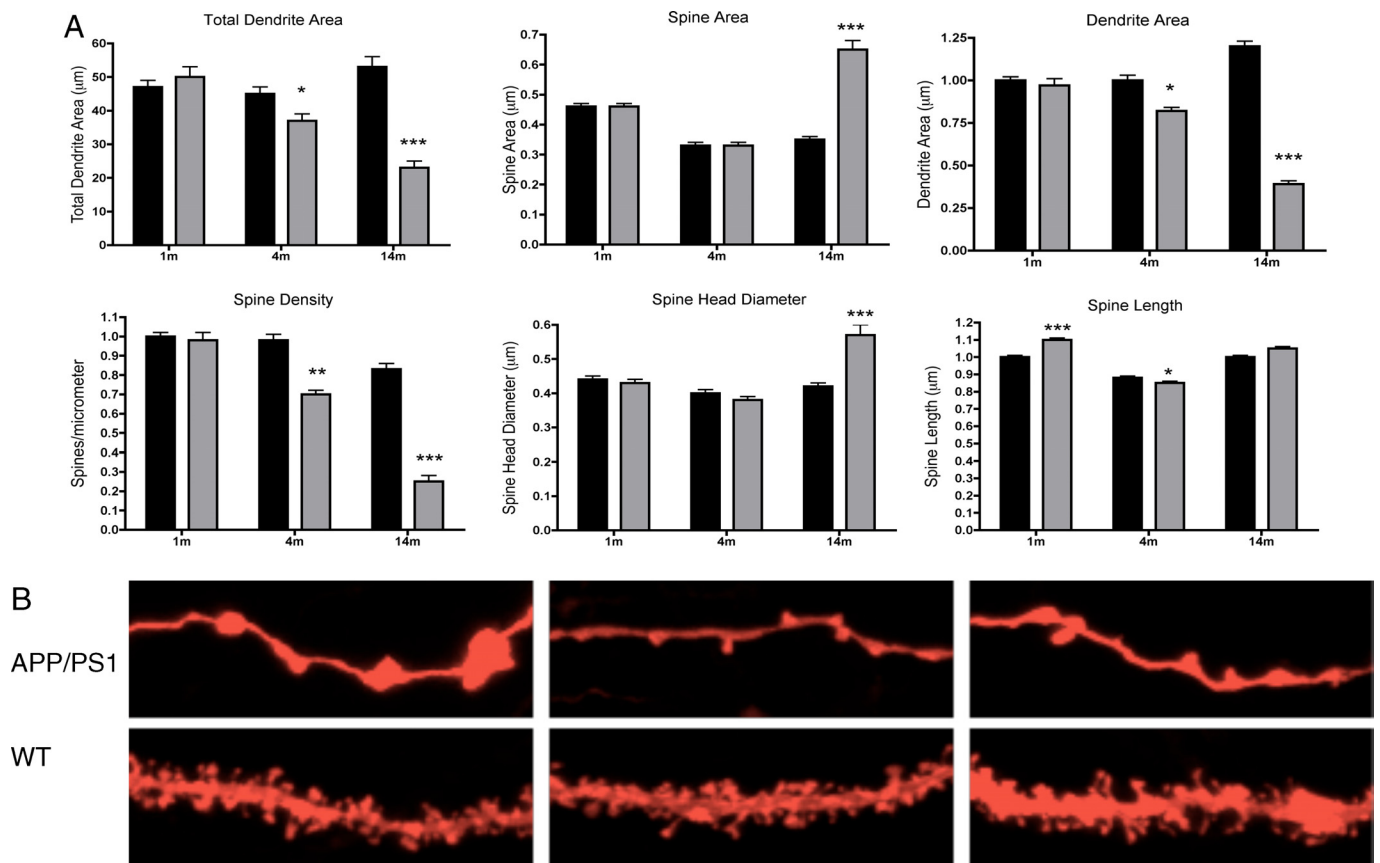
Fig. 3. Dendrite and spine alterations as a function of age in the APP/PS1 and WT mouse hippocampus. (*A*) APP/PS1 (black bars) and WT (gray bars) mice at 1, 4, and 14 months of age (three per genotype) were shot with DiI-labeled particles and subsequently quantified. An average of 16 dendritic segments were measured for each time point, per genotype, and a total of 2878 spine morphologies were measured (∗, $P < 0.05$, ∗∗, $P < 0.005$, ∗∗∗, $P < 0.0001$). (*B*) Examples of dendrite and spine morphologies of pyramidal hippocampal neurons used for quantification in 14-month-old APP/PS1 and WT mice. WT mice have considerably more spines than APP/PS1 mice, and total dendrite area and dendrite diameter are also increased in the WT animals. Although the transgenic animals have fewer spines, the remaining spines are larger. Scale, 10 μm.

In the present study, we show that the abnormalities in the dendritic architecture start at a relatively young age in the hippocampus of the APP/PS1 mouse with the appearance of dystrophic neurites and reduced spine density starting by 3 months of age. At 14–15 months of age, spines in APP/PS1 animals are less dense but have a larger head diameter than in controls, indicating fewer but stronger synapses. If this is an attempt by the organism to compensate for the loss of synapses by increasing strength of the remaining synapses, it is not sufficient to block the physiological and behavioral deficits in these animals.

In contrast to the changes in the hippocampus, no significant changes in dendritic morphology were found in the medium and large spiny neurons of the striatum of APP/PS1 mice compared with WT littermates. This is not surprising, as the striatum is relatively unaffected by degenerative changes in AD. There is no significant effect of rolipram or Uch-L1 on these neurons in WT mice.

Recent work from our laboratory has shown that LTP inhibition, whether the result of direct application of Aβ to hippocampal slices or the overproduction of endogenous Aβ in the slices from APP/PS1 double transgenic animals, can be blocked by treatment of the slices or, in the case of APP/PS1 trangenic animals, by systemic administration of either rolipram or a cell-permeant form of the enzyme ubiquitin c-terminal hydrolase L1 (V-Uch-L1) (34). Although there is no direct relationship between LTP and spine density, we asked whether these agents were capable of blocking or reversing the alterations in dendritic architecture induced by Aβ. Both rolipram and V-Uch-L1 were effective in ameliorating the

Aβ-induced effects in acute slices. In the intact APP/PS1 animal, the results obtained with the two compounds differ modestly. Whereas both agents restore spine density to values similar to those in WT animals, only rolipram increases spine head diameter and spine area at 3 months of age, although Uch-L1 does increase spine area and has a modest effect on spine head diameter at 15 months of age. This difference, which does not appear in the acute Aβ-treated slices, may reflect differences in the effective concentrations of the two agents in the brain as compared with their direct application in the bath. On the other hand, it could reflect differences in the behavioral consequences of treatment with these agents in which rolipram improves contextual fear learning the day after training, whereas Uch-L1 improves only the retention phase over time (34). This difference may be caused by the fact that rolipram raises intracellular levels of cAMP by blocking the activity of the cAMP degrading enzyme phosphodiesterase 4 whereas Uch-L1 does not alter cAMP levels. Both agents increase the activity of protein kinase A and the phosphorylation of the cAMP response element CREB.

The Aβ modulation of spine morphology involves the internalization and loss of AMPA and NMDA receptors from the spines (41, 42), the loss of debrin (42), and an increase in RhoA-GTP. The inhibition of PDE4 by rolipram or increased proteosome function after the elevation of Uch-L1 blocks these changes, but it is unclear whether the changes in intracellular levels of cAMP and Uch-L1 precede the alterations in the spines or are the consequences of them.
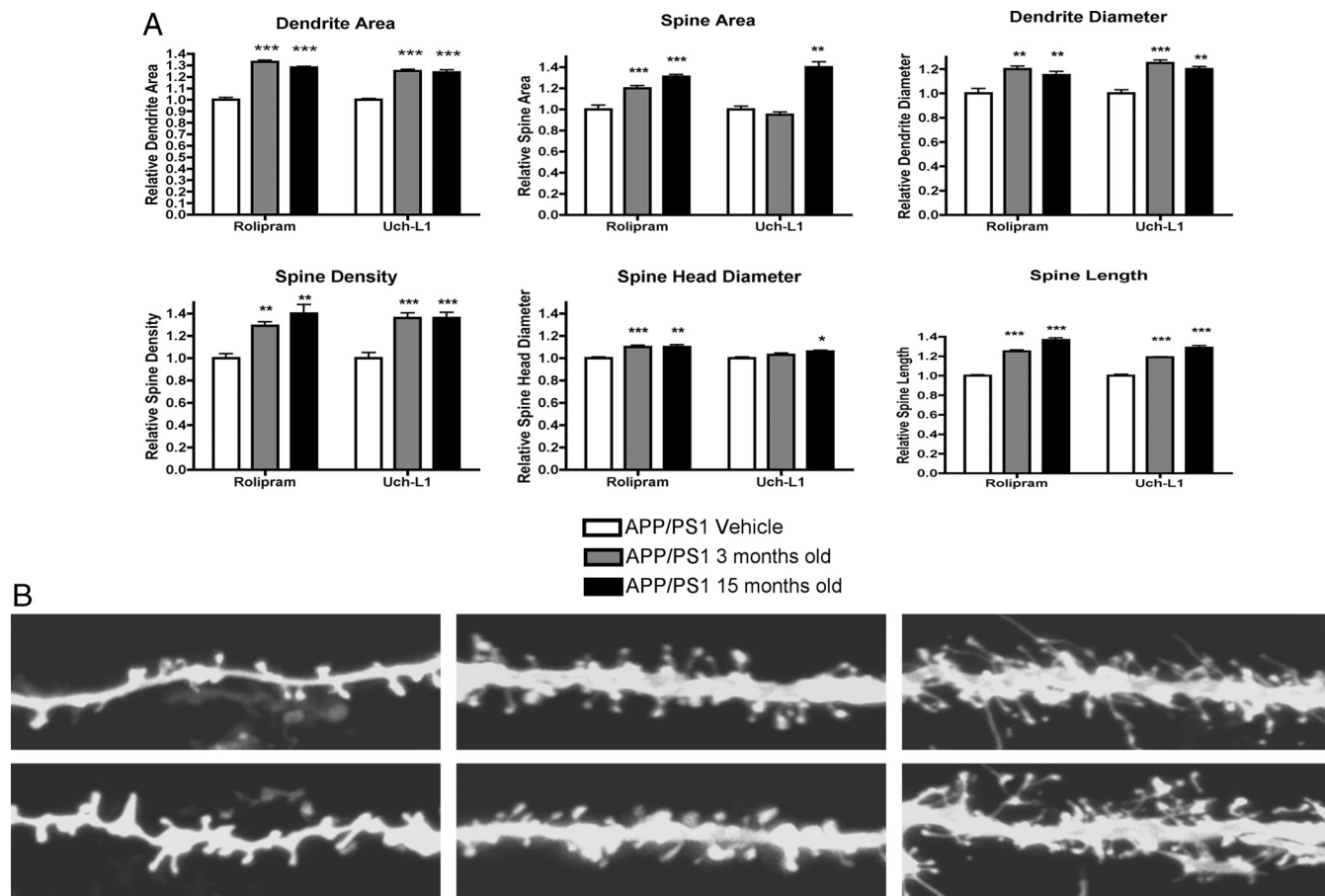
A

B

Fig. 4. *In vivo* treatment with V-Uch-L1 and rolipram reverse dendrite and spine pathologies in APP/PS1 mice. (*A*) Quantification graphs show that both rolipram and Uch-L1 significantly elevate total area and diameter of dendrites as well as density, area, length, and head diameter of spines. *, $P < 0.05$, **, $P < 0.005$, ***, $P < 0.0001$. Data were normalized by setting the vehicle control for each parameter equal to 1. (*B*) Examples of dendrite and spine morphologies of pyramidal hippocampal neurons used for quantification. Scale, 10 μm.

The fact that alterations in dendritic spine number and morphology, as well LTP and behavioral changes, are reversible long after their establishment in APP transgenic mice suggests that drugs that block these changes could be of therapeutic value. However, the models examined here lack key features of human AD, namely, tau alterations and cell death. This raises the possibility that the dendritic changes are prodromal and are a physical manifestation of the erosion of cognitive reserve, and that clinical AD occurs only when a point is passed where tau alterations and cell death commence. Even if this were the case, prevention of dendritic alterations would be likely to preserve cognitive function and to delay or block the development of irreversible changes. For drugs that block dendritic changes to have utility in the clinical context, we would require methods that allowed the early detection, either directly or by surrogate markers, of dendritic changes in living patients to guide in deciding whom to treat and when to treat them.

Methods

Transgenic Mouse Production. Double transgenic APP/PS1 mice were obtained by crossing hemizygous transgenic mice (HuAPP695SWE; line tg2576) expressing mutant human APP K670N, M671L (35) with hemizygous PS1 mice that express mutant human PS1M146V (line 6.2) (36). Transgenic mice were genotyped by polymerase chain reaction (PCR) using oligonucleotides for human APP and PS1 together with PuRe TaqPCR beads (Amersham 27–9559-01).

DiOlistic Labeling and Immunohistochemistry. DiOlistic labeling was performed as previously described (1, 37). Briefly, mice were anesthetized, then fixed with 4% paraformaldehyde by transcardiac perfusion. Their brains were removed and

sectioned coronally (300 μm) using a vibratome. Tissue sections were subsequently shot with DiI-coated particles using the Helios gene gun system (Bio-Rad).

Immunohistochemistry and DiOlistic labeling were combined to distinguish Aβ plaques and neuronal processes in transgenic mice, as described in Moolman et al. (27)). The 6E10 mouse anti-human Aβ antibody (SIGNET 9320–02) and A488 goat anti-mouse secondary fluorescent antibody (Molecular Probes A-21121) stained the Aβ plaques green. Sections were then shot with DiI-labeled bullets, which defined the neuronal architecture in red.

Acute Organotypic Hippocampal Slice Cultures. Organotypic hippocampal slice cultures were generated from WT or APP/PS1 mice. Mice were culled by cervical dislocation and their brains removed and placed in dissecting media (Dulbecco's Modified Eagle's Medium (MEM) with high glucose, L-glutamine, and 25 mM HEPES (GIBCO 21063–029). Hippocampi were dissected from the brain, and coronal 300 μm sections were cut using a McIlwain tissue chopper (Stolting). Slices were transferred to prewarmed Roth growth media (50% Dulbecco's MEM with high glucose, L-glutamine, and 25 mM Hepes (GIBCO 21063–029), 25% Hank's Balanced Salt Solution (GIBCO 24020–17), and 25% horse serum (GIBCO 16050–130), separated using spatulas and then placed on membranes (Millicell-CM 0.4 μm culture plate insert 12 mm diameter; Millipore TSTP04700) and incubated at 37 °C, 5% CO_2 for 90 min to recover.

After the recovery period, WT slices were treated with 100 nM oligomeric Aβ 1–42 (zcomAmerican Peptides 62–0-80 Lot Q04080 × 1), prepared as previously described (38). In the experiments described, rolipram and V-Uch-L1 were added at the same time as Aβ. The slices generated from APP/PS1 mice were treated in the same manner but without the addition of Aβ. Slices were left for 24 h at 37 °C, 5% CO_2, after which time they were fixed for 15 min in 4% paraformaldehyde and DiOlistic labeling performed.

Treatment of Slices with Rolipram and V-Uch-L1. Concentrations of rolipram (Sigma R6520) and V-Uch-L1 (TAT-HA-Uch-L1) were chosen based on our prior

PHYSIOLOGY

studies. Rolipram (1 μM) was found to promote the recovery of LTP in cultured hippocampal neurons treated with Aβ (19) and the same concentration to ameliorate deficits in LTP in APP/PS1 mice (7). A higher concentration of 10 μM rolipram was also tested. Rolipram was initially dissolved in DMSO, then diluted with H$_2$O and stored at −80 °C.

The cell-permeant form of ubiquitin c-terminal hydrolase L1 (V-Uch-L1) restores normal LTP in Aβ-treated slices and hippocampal slices from APP/PS1 mice at a concentration of 20 nM (34). V-Uch-L1 was prepared according to the protocol of Gong et al. (34), dissolved in 0.1 M phosphate-buffered saline (PBS), and stored at −80 °C.

In Vivo Treatments. APP/PS1 were s.c. injected with 0.03 mg/kg/day rolipram or V-Uch-L1 for 3 weeks at 3 months or 15 months of age. After 3 weeks of daily injection, two treated (drug-injected) and two untreated (vehicle-injected) APP/PS1 mice at each age were killed and DiOlistic labeling performed. The rolipram levels in the brain ranged from 0.6 μM to 2.0 μM at 30 min after injection. Wild-type 3-month-old mice were treated and analyzed in the same manner.

Microscopy. DiOlistically labeled neurons were imaged at high magnification (100X oil-immersion objective) using the Zeiss (LSM) 510 Meta confocal microscope. Images were magnified further using a ×3 zoom so that the mor-

phology of individual spines could be determined and subsequently quantified. Z stack images were collected at 0.3-μm intervals to cover the full depth of the dendritic arbors (20–30 μm) and then compressed into a single JPEG image.

Data Analysis. The ImageJ software program was used to quantify DiI-labeled neurons. Dendritic segments were chosen randomly from the apical and basal regions and were at least one soma's length away from the cell soma. Six parameters were measured, including total dendrite area, dendrite diameter, spine density, spine area, spine length, and spine head diameter. Figure 1 depicts the different parameters and explains how they were measured. All measurements were made with the investigator blinded to the genotype of the mouse and to the treatment used.

Statistical analysis was performed using the SPSS statistical package. At least 30 dendritic segments were photographed for each condition to provide statistically significant data. The nonparametric independent Mann-Whitney U test gave individual P values for comparisons, and Pearson rank correlations gave information on relationships between measurement parameters.

1. Mattson MP (2004) Pathways towards and away from Alzheimer's disease. *Nature* 430:631–639.
2. Price DL, Sisodia SS (1998) Mutant genes in familial Alzheimer's disease and transgenic models. *Annu Rev Neurosci* 21:479–505.
3. Wolfe MS, et al. (1999) Two transmembrane aspartates in presenilin-1 required for presenilin endoproteolysis and gamma-secretase activity. *Nature* 398:513–517.
4. Games D, et al. (1995) Alzheimer-type neuropathology in transgenic mice overexpressing V717F beta-amyloid precursor protein. *Nature* 373:523–527.
5. Holcomb L, et al. (1998) Accelerated Alzheimer-type phenotype in transgenic mice carrying both mutant amyloid precursor protein and presenilin 1 transgenes. *Nat Med* 4:97–100.
6. Gong B, et al. (2004) Persistent improvement in synaptic and cognitive functions in an Alzheimer mouse model after rolipram treatment. *J Clin Invest* 114:1624–1634.
7. Gonatas NK (1967) Neocortical synapses in a presenile dementia. *J Neuropathol Exp Neurol* 26:150–151.
8. Gonatas NK, Anderson W, Evangelista I (1967) The contribution of altered synapses in the senile plaque: An electron microscopic study in Alzheimer's dementia. *J Neuropathol Exp Neurol* 26:25–39.
9. Terry RD, et al. (1991) Physical basis of cognitive alterations in Alzheimer's disease: Synapse loss is the major correlate of cognitive impairment. *Ann Neurol* 30:572–580.
10. Hardy J, Selkoe DJ (2002) The amyloid hypothesis of Alzheimer's disease: Progress and problems on the road to therapeutics. *Science* 297:353–356.
11. Hsia AY, et al. (1999) Plaque-independent disruption of neural circuits in Alzheimer's disease mouse models. *Proc Natl Acad Sci USA* 96:3228–3233.
12. Mucke L, et al. (2000) High-level neuronal expression of abeta 1–42 in wild-type human amyloid protein precursor transgenic mice: Synaptotoxicity without plaque formation. *J Neurosci* 20:4050–4058.
13. Tsai J, Grutzendler J, Duff K, Gan WB (2004) Fibrillar amyloid deposition leads to local synaptic abnormalities and breakage of neuronal branches. *Nat Neurosci* 7:1181–1183.
14. Wu CC, et al. (2004) Selective vulnerability of dentate granule cells prior to amyloid deposition in PDAPP mice: Digital morphometric analyses. *Proc Natl Acad Sci USA* 101:7141–7146.
15. Cullen WK, Suh YH, Anwyl R, Rowan MJ (1997) Block of LTP in rat hippocampus in vivo by beta-amyloid precursor protein fragments. *Neuroreport* 8:3213–3217.
16. Freir DB, Holscher C, Herron CE (2001) Blockade of long-term potentiation by beta-amyloid peptides in the CA1 region of the rat hippocampus in vivo. *J Neurophysiol* 85:708–713.
17. Itoh A, et al. (1999) Impairments of long-term potentiation in hippocampal slices of beta-amyloid-infused rats. *Eur J Pharmacol* 382:167–175.
18. Vitolo OV, et al. (2002) Amyloid beta-peptide inhibition of the PKA/CREB pathway and long-term potentiation: Reversibility by drugs that enhance cAMP signaling. *Proc Natl Acad Sci USA* 99:13217–13221.
19. Nimchinsky EA, Sabatini BL, Svoboda K (2002) Structure and function of dendritic spines. *Annu Rev Physiol* 64:313–353.
20. Nusser Z, et al. (1998) Cell type and pathway dependence of synaptic AMPA receptor number and variability in the hippocampus. *Neuron* 21:545–559.
21. Matsuzaki M, et al. (2001) Dendritic spine geometry is critical for AMPA receptor expression in hippocampal CA1 pyramidal neurons. *Nat Neurosci* 4:1086–1092.
22. Murthy VN, Schikorski T, Stevens CF, Zhu Y (2001) Inactivity produces increases in neurotransmitter release and synapse size. *Neuron* 32:673–682.
23. Portera-Cailliau C, Pan DT, Yuste R (2003) Activity-regulated dynamic behavior of early dendritic protrusions: Evidence for different types of dendritic filopodia. *J Neurosci* 23:7129–7142.
24. Majewska A, Brown E, Ross J, Yuste R (2000) Mechanisms of calcium decay kinetics in hippocampal spines: Role of spine calcium pumps and calcium diffusion through the spine neck in biochemical compartmentalization. *J Neurosci* 20:1722–1734.
25. Gertz HJ, Cervos-Navarro J, Ewald V (1987) The septo-hippocampal pathway in patients suffering from senile dementia of Alzheimer's type. Evidence for neuronal plasticity? *Neurosci Lett* 76:228–232.
26. Takashima S, Ieshima A, Nakamura H, Becker LE (1989) Dendrites, dementia and the Down syndrome. *Brain Develop* 11:131–133.
27. Moolman DL, Vitolo OV, Vonsattel JP, Shelanski ML (2004) Dendrite and dendritic spine alterations in Alzheimer models. *J Neurocytol* 33:377–387.
28. Lanz TA, Carter DB, Merchant KM (2003) Dendritic spine loss in the hippocampus of young PDAPP and Tg2576 mice and its prevention by the ApoE2 genotype. *Neurobiol Dis* 13:246–253.
29. Shankar GM, et al. (2007) Natural oligomers of the Alzheimer amyloid-beta protein induce reversible synapse loss by modulating an NMDA-type glutamate receptor-dependent signaling pathway. *J Neurosci* 27:2866–2875.
30. Shrestha BR, et al. (2006) Amyloid beta peptide adversely affects spine number and motility in hippocampal neurons. *Mol Cell Neurosci* 33:274–282.
31. Alpar A, et al. (2006) Different dendrite and dendritic spine alterations in basal and apical arbors in mutant human amyloid precursor protein transgenic mice. *Brain Res* 1099:189–198.
32. Jacobsen JS, et al. (2006) Early-onset behavioral and synaptic deficits in a mouse model of Alzheimer's disease. *Proc Natl Acad Sci USA* 103:5161–5166.
33. Spires TL, et al. (2005) Dendritic spine abnormalities in amyloid precursor protein transgenic mice demonstrated by gene transfer and intravital multiphoton microscopy. *J Neurosci* 25:7278–7287.
34. Gong B, et al. (2006) Ubiquitin hydrolase Uch-L1 rescues beta-amyloid-induced decreases in synaptic function and contextual memory. *Cell* 126:775–788.
35. Hsiao K, et al. (1996) Correlative memory deficits, Abeta elevation, and amyloid plaques in transgenic mice. *Science* 274:99–102.
36. Duff K, et al. (1996) Increased amyloid-beta42(43) in brains of mice expressing mutant presenilin 1. *Nature* 383:710–713.
37. Gan WB, Grutzendler J, Wong WT, Wong RO, Lichtman JW (2000) Multicolor ''DiOlistic'' labeling of the nervous system using lipophilic dye combinations. *Neuron* 27:219–225.
38. Dahlgren KN, et al. (2002) Oligomeric and fibrillar species of amyloid-beta peptides differentially affect neuronal viability. *J Biol Chem* 277:32046–32053.
39. Desai NS, Cudmore RH, Nelson SB, Turrigiano GG (2002) Critical periods for experience-dependent synaptic scaling in visual cortex. *Nat Neurosci* 5:783–789.
40. Masliah E (1995) Mechanisms of synaptic dysfunction in Alzheimer's disease. *Histol Histopathol* 10:509–519.
41. Hsieh H, et al. (2006) AMPAR removal underlies Abeta-induced synaptic depression and dendritic spine loss. *Neuron* 52:831–843.
42. Lacor PN, et al. (2007) Abeta oligomer-induced aberrations in synapse composition, shape, and density provide a molecular basis for loss of connectivity in Alzheimer's disease. *J Neurosci* 27:796–807.

Smith et al.